

Thermal Chemistry of Methylene- and Phenyl-Functionalized Carbon Nanotubes

Janie Cabana, Stéphane Lavoie, and Richard Martel*

Regroupement Québécois sur les Matériaux de Pointe et département de chimie, Université de Montréal, Montréal, Canada

Received October 13, 2009; E-mail: r.martel@umontreal.ca

Abstract: Thermal desorption of covalently functionalized SWNT was followed using Raman, X-ray photoemission (XPS), and thermodesorption (TDS) spectroscopies. By functionalizing different sources of SWNT, we assess the thermal stability of phenyl- and methylene-SWNT derivatives in relation to the source diameter and helicity distribution. For all samples, broad desorption features were observed at ~600 K for the phenyl-SWNT and at ~500 K for the methylene-SWNT derivatives. In both cases, no influence on helicity and on diameter was observed for the range studied. The study shows that the stability of methylene addends on SWNT is inferior to that of the phenyl and proves that the main desorption pathway of phenyl addends is a phenyl–phenyl coupling reaction.

Introduction

The functionalization of single-walled carbon nanotubes (SWNT) is one of the most important tools available nowadays to modify the interaction of SWNT with their local environment.^{1,2} The covalent functionalization consists of grafting organic molecules to their sidewall, which creates SWNT derivatives having increased chemical functionalities, lower tendency to bundle up, and better dispersion capabilities in solution. These characteristics justify the development of covalent reactions to enable the processing and assembly of SWNT from solution. As examples of applications, studies have used covalent strategies for the assembly of nanotubes into electronic devices,^{3,4} the improvement of nanotube composites,^{5,6} and the development of new molecular probes.⁷

Because the grafting forms direct bonding to the sidewall, the covalent strategy alters the mechanical and electronic properties of SWNT. The most important changes are large decreases of their light emission⁸ and absorption⁹ properties and a drastic reduction of their electrical conductance.^{10,11} Such

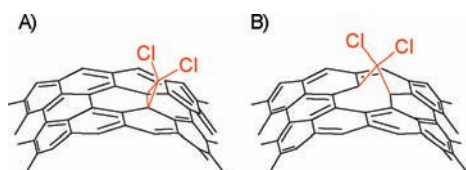
modifications are unfortunately detrimental to many applications. However, past reports have shown that the optical and electrical properties can be restored after annealing in a vacuum.^{3,12} Conductance measurements and Raman data have also revealed that the recovery of properties involves thermal defunctionalization reactions along with a sidewall reconstruction.¹³ The detail about this thermal chemistry is yet unclear, but the studies have revealed that the covalent approach, being mostly reversible, is an efficient tool for the processing of SWNT in solution.

Among the main covalent functionalizations of SWNT, the arenediazonium reaction draws special attention because of its efficiency and ease of implementation.¹⁴ It leads to highly functionalized phenyl-SWNT that can be subsequently used to attach a large variety of molecules. Thus, it enables, in only a few steps, one to tailor the surface properties of the nanotubes. Experiments have shown that the detachment of the phenyl addends occurs upon annealing between 400 and 700 K.¹³ To our knowledge, there is no detailed experimental study about this desorption process, although Margine et al. have recently explored the mechanism using ab initio calculations.¹⁵ As illustrated in Scheme 1, this theoretical study estimated a simultaneous detachment of phenyl pairs from the sidewall through a phenyl–phenyl coupling as the most probable pathway for desorption.

Another important class of sidewall reactions is the cycloaddition of carbenes. One of the most popular reactions, the dichlorocarbene cycloaddition, leads to a large number of dichloromethylene addends bridging two carbon atoms of the nanotube.¹⁶ Using ab initio calculations, it was predicted that

- (1) Niyogi, S.; Hamon, M. A.; Hu, H.; Zhao, B.; Bhowmik, P.; Sen, R.; Itkis, M. E.; Haddon, R. C. *Acc. Chem. Res.* **2002**, *35*, 1105–13.
- (2) Chen, J.; Hamon, M. A.; Hu, H.; Chen, Y.; Rao, A. M.; Eklund, P. C.; Haddon, R. C. *Science* **1998**, *282*, 95–98.
- (3) Klinke, C.; Hannon, J. B.; Afzali, A.; Avouris, P. *Nano Lett.* **2006**, *6*, 906–910.
- (4) Cabana, J.; Paillet, M.; Martel, R. *Langmuir*, **2010**, *26*, 607–612.
- (5) Xie, L.; Xu, F.; Qiu, F.; Lu, H.; Yang, Y. *Macromolecules* **2007**, *40*, 3296–3305.
- (6) Yang, K.; Gu, M.; Guo, Y.; Pan, X.; Mu, G. *Carbon* **2009**, *47*, 1723–1737.
- (7) Wu, W.; Wieckowski, S.; Pastorin, G.; Benincasa, M.; Klumpp, C.; Briand, J.; Gennaro, R.; Prato, M.; Bianco, A. *Angew. Chem., Int. Ed.* **2005**, *44*, 6358–6362.
- (8) Cognet, L.; Tsyboulski, D. A.; Rocha, J. R.; Doyle, C. D.; Tour, J. M.; Weisman, R. B. *Science* **2007**, *316*, 1465–1468.
- (9) Usrey, M. L.; Lippmann, E. S.; Strano, M. S. *J. Am. Chem. Soc.* **2005**, *127*, 16129–16135.
- (10) Hjort, M.; Stafstrom, S. *Phys. Rev. B* **2001**, *63*, 113406.
- (11) Wang, C.; Cao, Q.; Ozel, T.; Gaur, A.; Rogers, J. A. *J. Am. Chem. Soc.* **2005**, *11460*–11468.

- (12) Bahr, J. L.; Yang, J.; Kosynkin, D. V.; Bronikowski, M. J.; Smalley, R. E.; Tour, J. M. *J. Am. Chem. Soc.* **2001**, *123*, 6536–6542.
- (13) Cabana, J.; Martel, R. *J. Am. Chem. Soc.* **2007**, *129*, 2244–2245.
- (14) Dyke, C. A.; Tour, J. M. *J. Am. Chem. Soc.* **2003**, *125*, 1156–1157.
- (15) Margine, E. R.; Bocquet, M.; Blase, X. *Nano Lett.* **2008**, *8*, 3315–3319.
- (16) Chen, Y.; Haddon, R. C.; Fang, S.; Rao, A. M.; Eklund, P. C.; Lee, W. H.; Dickey, E. C.; Grulke, E. A.; Pendergrass, J. C.; Chavan, A.; Haley, B. E.; Smalley, R. E. *J. Mater. Res.* **1998**, *13*, 2423–2431.

Scheme 1. Proposed Mechanism by Margine et al. for the Detachment of Phenyl Addends from the SWNT Sidewall^a^a Adapted from ref 15.**Chart 1.** Different Configurations for the Methylene Addends: (A) the “Close Configuration” Defined with a Cyclopropyl Addend Formed with the Sidewall C–C Bond and (B) the “Open Configuration” in Which a Methylene Is Adsorbed on an Open Site Created by a Rupture of the Lattice C–C Bond

these addends can adopt two different configurations: the “close configuration” and the “open configuration”. The former is a cyclopropyl addend formed directly on top of the sidewall (Chart 1A), while the latter involves a ruptured C–C bond in the lattice as an open site to the methylene addend (Chart 1B).^{17,18} Of particular interest, the open configuration has been extensively studied by theory because it does not disturb the electrical conductance of the SWNT.^{19,20} Neither the stability of these configurations nor the reversibility of the cycloaddition reaction has been probed experimentally.

Herein, we performed a thermal desorption study of covalently functionalized SWNT. In this study, we compared the thermal stability of both the phenyl and the methylene SWNT derivatives and analyzed the desorption fragments. We concluded that the phenyl addends are the most stable thermally. In addition, we investigated the main desorption pathway of the phenyl derivatives and proved that the thermal reaction proceeds by direct phenyl–phenyl coupling mechanism. This is the first extensive experimental study on the thermal stability of two main classes of covalently functionalized SWNT.

Experimental Section

Iodophenyl and Phenyl Functionalization. In a typical experiment, SWNT (50.0 mg) and iodoaniline (3.0 g) or aniline (1.25 g) were added to a flask equipped with a reflux condenser and purged under nitrogen for 5 min. Isoamyl nitrite (2 mL) was then added via syringe, and the mixture was heated to 80 °C while being vigorously stirred. After 3 h, the resulting paste was diluted with DMF and filtered through a PTFE (0.45 μm) membrane (DMF, THF, propanol, water). The last step was repeated until no reactant was found in the solution using thin layer chromatography (TLC). Note that the solution was sonicated for 5 min between each filtration to increase the removal of the residual reagent.

Dichloromethylene Functionalization. Fifteen milligrams of SWNT was dispersed in 10 mL of SDS solution (0.1%) and

sonicated for 20 min in a bath. A condenser was then placed on the top of the flask, and 10 g of NaOH followed by 15 mL of chloroform were added slowly while stirring the solution. The solution was heated to 60 °C and left to react for 24 h. More reagents (chloroform (8 mL), NaOH (10 g), and water (8 mL)) were added to the mixture, and the reaction was pursued for another 48 h. At the end, the mixture was diluted in water and filtered through a PTFE membrane. The SWNT were cleaned by extraction (toluene/water) and filtration (DMF, CHCl₃, THF, propanol, water). Between each step, the solution was sonicated for 5 min to facilitate the removal of the residual reagent.

Annealing of SWNT Sample. When needed, the annealing of the sample was performed at 770 K under high-vacuum conditions at pressure below 5×10^{-5} Torr. The temperature was maintained for 45 min, then cooled slowly to room temperature before breaking the vacuum.

Characterization. The Raman spectra were acquired on thick deposits of SWNT on gold substrates using a Renishaw Invia MicroRaman spectrometer equipped with two laser lines at 632.8 and 785 nm wavelengths. The power density was adjusted to prevent heating. XPS measurements were carried out on thick deposits of SWNT on gold substrate using a VG ESCALAB 3 Mark II apparatus with a Mg K X-rays (1253.6 eV) operating at 15 KV and 20 mA.

SWNT deposited on a platinum substrate were used for conducting thermodesorption experiments (TDS). The thick deposits were obtained by the drop and dry technique using a THF solution of SWNT. The SWNT suspension was composed of large agglomerates. During TDS, the pressure was kept below 10^{-7} Torr, and the mass spectrometer was set to detect a small selection of mass to charge ratios within the range from 1 to 100 u/e (i.e., spectrometer maximum). Each sample was heated at 400 K for 5 min before TDS. This pretreatment was found necessary to remove excess of solvent trapped in the sample. TGA-MS experiments were done using a TGA-MS from TA Instruments. Approximately 2 mg of SWNT powder was used for each experiment, and the heating rate was 10 °C/min under nitrogen flow. The experiment was repeated three times.

Results and Discussion

Phenyl Derivatives. Three sources of SWNT covalently functionalized with iodophenyl or phenyl moieties have been studied: purified HipCo SWNT (HipCo SWNT) from Carbon Nanotechnologies Inc., CoMoCat SWeNT purified (CoMoCat SWNT, lot SG0000007) from SouthWest Nanotechnologies, and laser ablation SWNT (LA SWNT) donated by B. Simard from the National Research Council of Canada. No further purification of the SWNT has been made. The densities of iodophenyl addends grafted onto the sidewalls, estimated by X-ray photoelectron spectroscopy (XPS) using the intensity of the I3d5 and the C1s peak, were 1 iodophenyl for every 50 carbons for the HipCo SWNT and 1 iodophenyl for every 12 carbons for the CoMoCat SWNT (see the Supporting Information).

Figure 1 presents the Raman spectra at 632.8 nm light excitation of HipCo and CoMoCat SWNT taken from (a,d)

(17) Li, R.; Shang, Z.; Wang, G.; Pan, Y.; Cai, Z.; Zhao, X. *J. Mol. Struct. (THEOCHEM)* **2002**, *583*, 241–247.

(18) Bettinger, H. F. *Chem.-Eur. J.* **2006**, *12*, 4372–4379.

(19) Lee, Y.; Marzari, N. *Phys. Rev. Lett.* **2006**, *97*, 116801.

(20) López-Bezanilla, A.; Triozon, F.; Latil, S.; Blase, X.; Roche, S. *Nano Lett.* **2009**, *9*, 940–944.

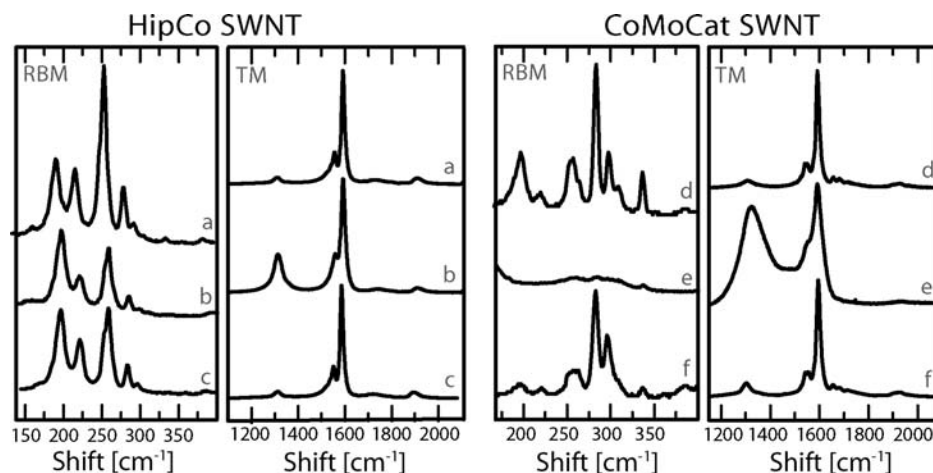


Figure 1. Raman spectra at 632.8 nm laser excitation of the HipCo and CoMoCat SWNT for, respectively, (a,d) the pristine; (b,e) the iodophenyl-SWNT; and (c,f) the iodophenyl-SWNT after an annealing at 770 K. Note, for better clarity, the radial breathing mode (RBM) region was normalized with the intensity of the band at 195 cm^{-1} for the HipCo sample and at 285 cm^{-1} for the CoMoCat sample. No signal could be seen for functionalized CoMoCat samples. The region of the tangential modes (TM) is composed of the D-band ($1310\text{--}1320\text{ cm}^{-1}$) and the G-bands ($1540\text{--}1590\text{ cm}^{-1}$), and the intensity was normalized with respect to the G-band maximum.

pristine, (b,e) functionalized with iodophenyl, and (c,f) defunctionalized samples. At first sight, the Raman spectroscopy provides a fast and direct evidence of the functionalization of the sidewalls.²¹ During the functionalization, the sp^2 hybridization of the carbons of the sidewall is changed to sp^3 after bonding to phenyl moieties. It increases the bond angle and forms a structural distortion that alters the electronic structure of the SWNT.²² As seen in Figure 1, this deformation modifies significantly the Raman spectra. These modifications are a general loss of intensity, a broadening of both the D-band and the G-bands, and an increase of the D-/G-band ratio.^{21,23} All of those features can be observed in Figure 1b for the HipCo SWNT and in Figure 1e for the CoMoCat SWNT samples. By comparing the spectra in the $1200\text{--}2000\text{ cm}^{-1}$ region, it appears that the spectrum of the functionalized CoMoCat SWNT is more affected by the reaction, a feature that is consistent with the higher density of addends measured by XPS on these samples. The relative intensities of the radial breathing mode (RBM) are also modified by the grafting of phenyl addends. A variation in the signal between RBM modes somehow suggests that the reactivity of the nanotube further depends on the nanotube helicity, which is in agreement with other studies.²⁴ In the case of the CoMoCat sample, the higher level of functionalization induces a major loss of the RBM bands (Figure 1e).

The annealing of the functionalized nanotubes at 770 K leads to the modification of the Raman spectra, as seen in Figure 1c and f. The thermal treatment induces the detachment of the addends from the nanotube sidewall¹³ and triggers the reconstruction of the lattice back to its original honeycomb structure. This regeneration leads to a decrease of the D-/G-band ratio and an increase of the RBM bands. Moreover, further observations can be obtained by comparing spectra of pristine (Figure 1a,d) with those of defunctionalized SWNT (Figure 1c,f). First,

the D-/G-band ratio remains slightly higher in the defunctionalized sample (12% of rise for the HipCo and 40% for the CoMoCat), and, second, the relative intensities of the RBM bands are not the same. These features can be explained by the occurrence of a small number of structural defects following the defunctionalization process. Such damage has been previously identified using electric measurements and found to be irreversible, even if further annealing is performed at 920 K.¹³ In the HipCo sample, the relative intensity of the RBM band at 257 cm^{-1} was altered the most by the reaction (Figure 1b) and is still modified the most after the annealing (Figure 1c). Therefore, it suggests that the damage induced by reaction/annealing processes is proportional to the yield of the functionalization.

To study more extensively the thermal stability of the iodophenyl-SWNT, thermodesorption spectroscopy was performed on thick layers of SWNT deposited on a platinum disk. The intensity of several mass/charge ratios (m/e) was followed during the thermal defunctionalization of the SWNT. Top and bottom spectra of Figure 2 present typical variations in intensity of $m/e = 77$ with the temperature (heating rate of 1 K/s) for the iodophenyl-HipCo and iodophenyl-CoMoCat SWNT samples, respectively. The mass 77 fragment corresponds to phenyl cations, which is one of the key desorption fragments. A preheating treatment at 400 K was necessary to remove the majority of the residual organic solvent trapped in the sample.

Both TDS spectra show an important desorption peak at around 600 K. Although the maxima of desorption occur at the same temperature, the peaks have different line shapes, and the broader is from the CoMoCat SWNT. The detachment of iodophenyl was further confirmed by XPS analysis using the relative intensity of the I3d5 peak measured at different temperatures. No iodine signal could be detected in the SWNT samples after an annealing at 770 K. Moreover, to ensure that the intensity around 600 K originates from the functional groups, TDS spectra of pristine HipCo and CoMoCat SWNT were also recorded (see the Supporting Information). No desorption was observed at 600 K in these cases.

The HipCo and CoMoCat sources have different nanotube populations and thus allow us to extract information about

(21) Graupner, R. *J. Raman Spectrosc.* **2007**, 673–683.

(22) Zhao, J.; Park, H.; Han, J.; Lu, J. P. *J. Phys. Chem. B* **2004**, 108, 4227–4230.

(23) Fantini, C.; Usrey, M. L.; Strano, M. S. *J. Phys. Chem. C* **2007**, 111, 17941–17946.

(24) Strano, M. S.; Dyke, C. A.; Usrey, M. L.; Barone, P. W.; Allen, M. J.; Shan, H.; Kittrell, C.; Hauge, R. H.; Tour, J. M.; Smalley, R. E. *Science* **2003**, 301, 1519–1521.

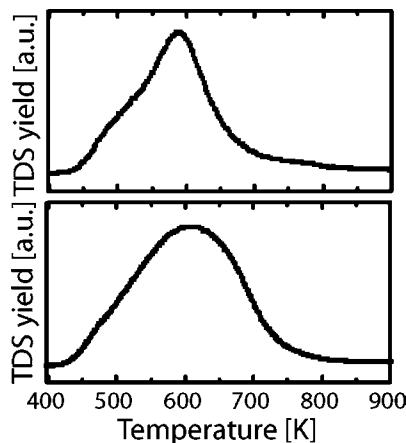


Figure 2. Thermodesorption spectra ($m/e = 77$) of iodophenyl-functionalized HipCo SWNT (top) and CoMoCat SWNT (bottom) with a heating rate of 1 K/s and a pressure below 10^{-7} Torr.

the dependence of the thermal stability on diameter and helicity. The CoMoCat sample has a narrow distribution of helicity given that about 57% of the semiconducting tubes have (6,5) or (7,5) chiralities.²⁵ Its average diameter is also smaller, that is, 0.81 nm as compared to 0.93 nm for the HipCo nanotubes.²⁶ Nonetheless, both TDS spectra present similar maximum desorption rates located at around 600 K. Therefore, within the experimental error, the difference in the sample helicity and diameter distributions does not influence the overall defunctionalization process. There is, however, a significant difference in peak width between the two systems. We speculate that this is mainly due to the different microstructures (porosity and density) of the deposits. This is reasonable because the dispersion and exfoliation in organic solvents are complex processes that depend on parameters such as nanotube diameter, length distribution, purity, and concentration in the solution.^{27–29} Furthermore, desorption characteristics of molecules physisorbed on SWNT have been found to depend on the availability of the different adsorption sites (e.g., groove of a bundle versus surface of the deposit).^{30–32} This further influences the desorption kinetics and modifies the peak shapes in TDS. Similar phenomena seem probable during the desorption of chemisorbed molecules.

To verify the mechanism of defunctionalization proposed by Margine et al.¹⁵ (Scheme 1), phenyl-SWNT were annealed in a TGA-MS apparatus, and the intensity of both gaseous phenyl and biphenyl cations was monitored. The TDS instrument was not used because of the detection limit of our mass spectrometer

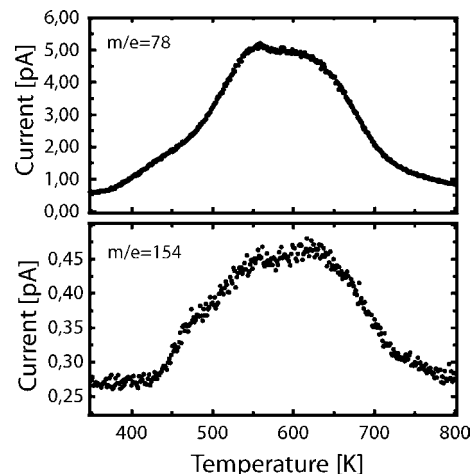


Figure 3. TGA-MS spectra of the fragment $m/e = 78$ (top) and $m/e = 154$ (bottom) from the phenyl-functionalized LA SWNT. The experiment was done under nitrogen (90 mL/min) at a heating rate of 10 K/min.

(Balzer). Unsubstituted phenyl was used as addends instead of iodophenyl to maximize the intensity of the possible biphenyl cation ($m/e = 154$). The full characterization of the phenyl functionalized LA SWNT used in this experiment can be found in the Supporting Information.

The desorption spectra in Figure 3 give a formal proof of the coupling mechanism illustrated in Scheme 1. This is the key finding of our study and confirms the prediction made by Margine et al.¹⁵ The presence of both the 78 m/e and the 154 m/e fragments indicates phenyl and biphenyl cations desorption at around 600 K. The TDS peak of the phenyl cations, although more intense, is simultaneous to the one of the biphenyl cations.

In their ab initio study of the reaction pathways, Margine et al.¹⁵ had found a significant difference in the temperature of desorption of phenyl versus biphenyl molecules from the nanotube sidewall. On the basis of this theoretical result and of the simultaneous observation of the desorption of $m/e = 78$ and $m/e = 154$, it is possible to conclude that biphenyl desorption is the main reaction path and that the phenyl fragments observed come from the fragmentation of biphenyl in the mass spectrometer. A coupling in the gas phase of the phenyl radicals can be ruled out because the desorption occurs in a strong flow of nitrogen, and their concentration would therefore be extremely low.

This experiment also supports the conclusion that the diameter of the SWNT does not influence the temperature of desorption. Indeed, LA SWNT have an average diameter (1.3 nm)³³ considerably larger than the CoMoCat and the HipCo SWNT; yet the TDS peak is found to be similarly located at around 600 K.

Methylene Derivatives. The covalent functionalization of HipCo and CoMoCat SWNT with dichloromethylene moieties was achieved via a dichlorocarbene cycloaddition.¹⁶ The degree of functionalization has been determined using the intensity of Cl2p and C1s peaks in the XPS spectra. It was estimated that 1 out of 72 carbon atoms and 1 out of 77 carbon atoms have reacted for HipCo SWNT and CoMoCat SWNT, respectively.

The Raman spectra of the pristine (a,d), methylene-functionalized (b,e), and methylene-defunctionalized SWNT (c,f) are

- (25) Bachilo, S. M.; Balzano, L.; Herrera, J. E.; Pompeo, F.; Resasco, D. E.; Weisman, R. B. *J. Am. Chem. Soc.* **2003**, *125*, 11186–11187.
- (26) Bachilo, S. M.; Strano, M. S.; Kittrell, C.; Hauge, R. H.; Smalley, R. E.; Weisman, R. B. *Science* **2002**, *298*, 2361–6.
- (27) Bahr, J. L.; Mickelson, E. T.; Bronikowski, M. J.; Smalley, R. E.; Tour, J. M. *Chem. Commun.* **2001**, 193–194.
- (28) Furtado, C. A.; Kim, U. J.; Gutierrez, H. R.; Pan, L.; Dickey, E. C. *J. Am. Chem. Soc.* **2004**, *126*, 6095–6105.
- (29) Bergin, S. D.; Sun, Z.; Rickard, D.; Streich, P. V.; Hamilton, J. P. *ACS Nano* **2009**, *3*, 2340–2350.
- (30) Kondratyuk, P.; Wang, Y.; Johnson, J. K.; Yates, J. T. *J. Phys. Chem. B* **2005**, *109*, 20999–21005.
- (31) Ulbricht, H.; Zacharia, R.; Cindir, N.; Hertel, T. *Carbon* **2006**, *44*, 2931–2942.
- (32) Komarneni, M.; Sand, A.; Goering, J.; Burghaus, U. *Chem. Phys. Lett.* **2009**, *473*, 131–134.

- (33) Kingston, C. T.; Jakubek, Z. J.; Denommée, S.; Simard, B. *Carbon* **2004**, *42*, 1657–1664.

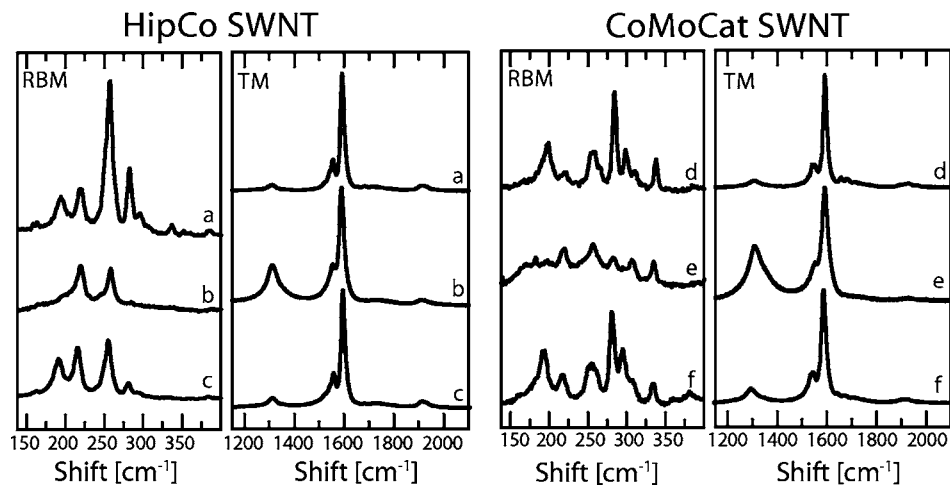


Figure 4. Raman spectra at 632.8 nm wavelength excitation of HipCo and CoMoCat SWNT. (a,d) Pristine SWNT; (b,e) dichloromethylene-functionalized SWNT; and (c,f) dichloromethylene-functionalized SWNT after an annealing at 770 K. The region of the radial breathing mode (RBM) is normalized with the intensity of the band at 220 and at 257 cm^{-1} for the HipCo and CoMoCat samples, respectively. The region of the tangential modes (TM) is dominated by the D-band (1310–1320 cm^{-1}) and the G-bands (1540–1590 cm^{-1}), and the intensity was normalized with respect to the G-band maximum.

presented in Figure 4 for both the HipCo and the CoMoCat samples. Similar to the grafting of iodophenyl moieties, the grafting of dichloromethylene addends leads to changes in the Raman spectra that include a broadening of the D- and G-bands, an augmentation of the D-/G-band ratio, and a modification of the relative intensities of the RBM. Note that the RBM region in Figure 4a is slightly different from the one presented in Figure 1a. This is explained by the use of a different batch of HipCo SWNT for the methylene functionalization than the one used for the phenyl functionalization. Also, the RBM of the functionalized CoMoCat are visible, which was not the case for the iodophenyl-CoMoCat presented in Figure 1e. This is explained by a degree of functionalization that is 85% lower, as determined by XPS.

After an annealing at 770 K, the relative intensity of the D-/G-band ratio decreases, while it increases for the RBM bands for both the CoMoCat and the HipCo samples. The resulting D-/G-band ratio presented a 50% rise in the HipCo sample and a 68% rise in the CoMoCat sample, as compared to the one in the pristine nanotubes. Those relative percentages of increase are higher than for the phenyl derivatives, which were 12% and 40%. However, in both cases, most of the damage induced by the functionalization was removed.

The thermal stability of the dichloromethylene-SWNT was studied by TDS using the same conditions as for the iodophenyl-SWNT. Figure 5 presents the intensities of the CCl^+ fragment ($m/e = 47$) monitored with temperature at a heating rate of 1 K/s. The spectra of the pristine HipCo SWNT and CoMoCat SWNT were also measured as a reference to make sure that the TDS spectra originated from the desorption of the addends. These spectra can be found in the Supporting Information.

Both TDS spectra of the dichloromethylene-HipCo and dichloromethylene-CoMoCat SWNT show an important peak of desorption at around 500 K. The desorption temperature is ~ 100 K lower than that of the iodophenyl-SWNT, which is significant as compared to our experimental uncertainty (about 20 K). The dichloromethylene derivatives are therefore less stable than the iodophenyl derivatives. This result is consistent with the *ab initio* study made by Margine et al.¹⁵ showing a smaller binding energy and activation energy of desorption for the dichloromethylene in open configuration than for the

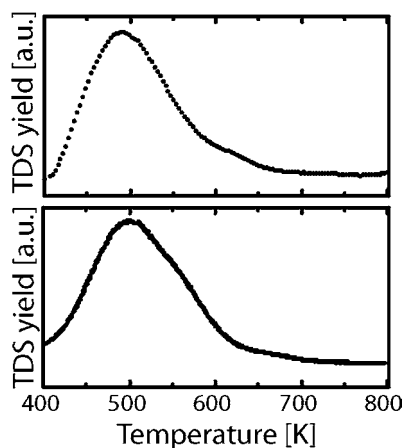


Figure 5. Thermodesorption spectra ($m/e = 47$) of the dichloromethylene-functionalized HipCo SWNT (top) and the dichloromethylene-functionalized CoMoCat SWNT (bottom) with a heating rate of 1 K/s and a pressure below 10^{-7} Torr.

desorption of biphenyl. However, in the present study, the configuration of the methylene addends (open or close) could not be determined. In addition, as for the phenyl addends, the differences in helicity and diameter populations (ϕ_{mean} : 0.81 nm versus 0.93 nm) between the HipCo and CoMoCat samples do not lead to an apparent variation in the desorption temperature. This result is unexpected because numerous theoretical works have demonstrated that the binding energy of a methylene addends depends on the curvature and on the angle between the grafting site and the nanotube axis.^{17–19} Furthermore, Margine et al.¹⁵ have calculated that the desorption barrier of a small SWNT is higher than the one of a large diameter SWNT (approximated as a graphene sheet). As such, differences in the TDS spectra between the CoMoCat and the HipCo sample were expected. The reason for the absence of such feature is most likely due to the limited diameter range studied and the low sensitivity of our measurements to detect small variation of the desorption energy. Another possibility would involve diffusion

of the methylene addends on the sidewall toward a preferable site just prior to their desorption.

Conclusion

We determined the temperature of defunctionalization of iodophenyl- and dichloromethylene-SWNT. The phenyl derivatives were found to be more stable, with a maximal rate of desorption at 600 K, that is, 100 K higher than for the methylene addends. The temperature of defunctionalization was found to be the same for the helicity and diameter distributions considered in this study. Moreover, we proved experimentally that the detachment of the phenyl addends occurs through a phenyl–phenyl coupling at the sidewall. All of our results agree with recent theoretical predictions made by Margine et al.¹⁵

While the determination of the thermal stability of these covalent derivatives represents a key parameter to consider when developing new SWNT composites, the present study provides further understanding of the chemistry of SWNT defunctionalization, and the results will guide the use of covalently functionalized nanotubes in future applications.

Acknowledgment. We thank Professor P. McBreen for giving access to the TDS apparatus, B. Simard from the National Research Council of Canada for providing carbon nanotubes, and François Lapointe for a critical reading of the manuscript. J.C. and S.L. acknowledge the receipt of a FQRNT postgraduate fellowship and a NSERC postdoctoral fellowship, respectively. Part of the work was carried out the Central Facilities of École Polytechnique and Université de Montréal. This project is supported by the National Sciences and Engineering Research Council of Canada (NSERC) and the Canada Research Chair (CRC).

Supporting Information Available: Raman spectra at 785 nm light excitation of HipCo and CoMoCat SWNT for pristine, iodophenyl functionalized, iodophenyl defunctionalization, dichloromethylene functionalized, and dichloromethylene defunctionalized. Raman at 632.8 nm of pristine- and phenyl-functionalized LA SWNT. Also, XPS analysis of iodophenyl- and dichloromethylene-functionalized HipCo and CoMoCat SWNT. TDS spectra of pristine HipCo and CoMoCat SWNT using $m/e = 47, 77$. This material is available free of charge via the Internet at <http://pubs.acs.org>.

JA908729Y